

1 **CO₂-Based Heavy Oil Recovery Processes for Post-CHOPS Reservoirs**

2
3 Amin Sharifi Haddad¹ and Ian Gates^{2*}

4
5 ¹The School of Engineering
6 University of Aberdeen

7
8 ²Department of Chemical and Petroleum Engineering
9 Schulich School of Engineering
10 University of Calgary

11 **Abstract**

12 Cold Heavy Oil Production with Sand (CHOPS) is currently the process of choice for recovery
13 from unconsolidated solution-gas rich heavy oil reservoirs. Compared to waterflood and thermal
14 recovery processes, primary processes such as CHOPS have relatively low energy and emission
15 intensities; in other words, they can be considered as relatively ‘clean’ fossil fuel energy
16 recovery processes. However, with recovery factors between 5 and 15% at the end of its
17 economic life, there is a search for follow-up processes that yield additional oil from these
18 reservoirs with continued low energy and emission intensities. One option is CO₂-based
19 enhanced oil recovery (EOR) processes – CO₂ can lower oil viscosity and if some fraction of the
20 injected CO₂ is sequestered in the reservoir, then the process can be considered a CO₂ storage
21 process in addition to an oil follow-up recovery process. Here, we evaluate the energy return and
22 CO₂ sequestered in cyclic CO₂ and cyclic CO₂-hot water injection processes in a post-CHOPS
23 heavy oil field. The results reveal that overall recovery factors can be raised through appropriate
24 design of the CO₂ follow-up process. Cyclic CO₂ injection achieves an incremental 2.4%
25 recovery factor (over 4 years of operation) with high energy return ratio whereas CO₂-hot water
26 processes achieve higher recovery factors with lower energy return ratios. In these processes, the
27 amount of CO₂ that remains sequestered in the reservoir is small, typically less than 5%. Thus,
28 these EOR processes are not strong candidates for CO₂ sequestration.

29 **Keywords:** heavy oil; cold production of heavy oil with sand; post-CHOPS; CO₂ injection;
30 follow-up recovery processes

31 *Corresponding author:

Ian D. Gates

32 Email: ian.gates@ucalgary.ca

33 Tel No: +1(403)-220-5752; Fax No: +1(403)-284-4852

34

35 **1. Introduction**

36 Primary production of heavy oil resources, often referred to as cold production, is attractive due
37 to low operating and capital costs of wells and surface equipment. Another key benefit of these
38 heavy oil recovery processes is that their energy intensity (net energy consumed per unit oil
39 produced, 4 GJ/m³ oil), greenhouse gas (GHG) emissions intensity (typically less than 300-400
40 kgCO₂eq/m³ oil), and water consumption (net gain of water) are all better than thermal extra
41 heavy oil recovery processes such as Cyclic Steam Stimulation (CSS) and Steam-Assisted
42 Gravity Drainage (SAGD) [32]. For example, in SAGD, the energy intensity is typically between
43 6-12 GJ/m³ oil, GHG emissions intensity 500-1,500 kgCO₂eq/m³ oil, and water consumption is
44 100-250 kg/m³ oil (assuming steam-to-oil ratio between 2 and 5 m³/m³ and 95% water recycle)
45 [15]. Thus, on a per volume basis, heavy oil cold production processes have significant energetic
46 and emissions advantages over that of thermal processes. In Western Canada, about 80% of
47 heavy oil resources are found in reservoirs <5 m thick which due to its high viscosity (1,000-
48 35,000 cP), low solution gas to oil ratio (GOR, ~8-15 m³/m³), and low initial reservoir pressures,
49 have primary recovery factors from 3 to 8% [1]. In some cases, if the solution gas content is high
50 enough and there are no neighbouring water zones, recovery factors reach as high as 15% [19]; 3
51 to 15% recovery factor is typical of primary production of heavy oil worldwide [27-29].

52 Several studies have been conducted to understand mechanisms of heavy oil production
53 processes including experimental studies on sand production and foamy oil flow behavior, for
54 example, Tremblay et al. [27-29], and Maini et al. [21, 22] among others. Also, due to sand
55 production, as the process evolves, wormholes are created within the reservoir [29]. The
56 wormholes are believed to be of order of a few tens of centimeters in diameter and they extend
57 up to several hundred meters into the reservoir. There are several CHOPS wormhole models in

58 the literature, for example [11, 18, 26]. The key challenge faced by operators after CHOPS has
59 been done is that the reservoir is permeated with wormholes which often connect wells together.
60 This means that injected fluid moves through the wormholes with little contact with the reservoir
61 bypassing the heavy oil-laden reservoir between the wormholes. In heavy oil reservoirs where
62 CHOPS has not been operated, currently secondary recovery process such as water and polymer
63 flooding are used which work effectively in reservoirs where the heavy oil viscosity is less than
64 ~5,000 cP [5, 9]. Water flooding and polymer flooding in post-CHOPS reservoirs suffer from the
65 existence of the high permeability wormholes and gas-saturated zones that lead to low
66 displacement and sweep efficiencies and thus low incremental recovery factor [1, 23, 25].

67 Another injectant that can be considered is carbon dioxide – it can act both as a solvent to lower
68 the heavy oil viscosity as well as a swelling agent that expands the oil phase volume within pores
69 [20]. Also, there are environmental benefits if some fraction of the CO₂ is sequestered within the
70 reservoir. At this point, there are no detailed studies on the use of CO₂ as an injectant for post-
71 CHOPS reservoirs for incremental recovery of oil and to evaluate the capability of the processes
72 to sequester CO₂. In this study, we evaluate the use of CO₂ and CO₂-hot water mixtures for
73 enhanced oil recovery from a post-CHOPS reservoir as well as the processes' ability to sequester
74 CO₂.

75 For heavy oil reservoirs, waterflooding has shown very poor performance [1, 23]. Miller's study
76 of different water flood operations in Western Canadian heavy oil reservoirs along with his
77 theoretical investigations showed that waterflooding has very poor sweep efficiency due to the
78 adverse mobility ratio, heterogeneity of the reservoirs, and presence of wormholes [23]. He
79 found that by using horizontal wells, hot water injection, and steam stimulation may not
80 consistently improve process performance. In polymer (aqueous polymer solution) injection, the

81 mobility ratio of the water and oil is improved which prevents viscous fingering. This strategy is
82 used by some companies in western Canadian heavy oil reservoirs e.g. in the Pelican Lake
83 project operated by Canadian Natural Resources Limited and the Brintnell polymer flood
84 operated by Cenovus. Laboratory studies of polymer flooding and alkaline/surfactant flooding
85 reveal small increases of recovery factor from heavy oil reservoirs [3, 16, 20, 23]. However, field
86 results have not confirmed this improvement in Western Canadian reservoirs [23]. Dong et al.
87 [12] conducted laboratory experiments to produce heavy oil through an alkaline/surfactant
88 recovery process which ended up with total recovery factors up to 20%.

89 Gates [14] investigated the application of solvent-aided SAGD in thin (8 m) oil sands reservoirs.
90 The results revealed that lower steam usage and net injected energy-to-oil ratio are possible
91 compared to the traditional SAGD process. SAGD and its derivatives are vulnerable to excessive
92 heat losses to the overburden and understrata. Investigations on in situ combustion (ISC) have
93 been performed through laboratory, modeling and pilot tests for heavy oil and oil sands thermal
94 recovery, however, ISC has not yet enjoyed the success of other thermal methods such as SAGD
95 and CSS due to complexity of reaction kinetics and control of the process [4]. Application of ISC
96 as a follow-up process for CHOPS reservoirs was proposed recently by Chen et al. [8]. Their
97 experiments show promising results (recovery factors >50%) at the laboratory scale. However,
98 ISC has not been tested in the field in post-CHOPS reservoirs.

99 Solvent-based processes have been tested for oil sands reservoirs and demonstrated good
100 recovery factors. These types of processes can be expanded to CHOPS reservoirs. Zhao et al.
101 [32] conducted an optimization analysis for solvent-aided steam-flooding strategy for a 4 m thick
102 heavy oil reservoir. Their results demonstrated that steam-solvent optimization can improve the
103 process performance compared to injection pressure optimization only. They also performed a

104 comparative simulation study to find a viable thermal recovery process for recovery in a thin
105 (<5m) heavy oil reservoir [31]. Their investigation revealed that SAGD and steam flooding
106 would not be efficient options for thin heavy oil reservoirs due to their high cumulative energy
107 injected-to-oil ratio (cEOR >13.6 GJ/m³). They concluded that hot water injection is possible
108 with cEOR ranging from 8 to 14 GJ/m³ although this is high relative to the cold production
109 process. Recent studies suggest that there is potential for cyclic solvent injection for thin heavy
110 oil reservoirs [25-28]. Chang and Ivory [7] used a specific well configuration for solvent
111 injection (CO₂, CH₄, C₃H₈) as follow-up processes for CHOPS reservoirs. They used vertical
112 injectors and a horizontal producer at lower depth below the bottom hole location of the CHOPS
113 vertical wells. In these recovery processes, oil production mechanisms are dilution (lowers oil
114 phase viscosity) and gravity-viscous flow. Different operation scenarios revealed how
115 wormholes can increase the recovery factor or inappropriate design reduces the oil rate recovery
116 due to solvent bypassing the reservoir through wormholes. Huerta et al. [17] performed an
117 experimental study on the use of acid gas (CO₂/H₂S) as solvent for cyclic solvent injection in
118 heavy oil reservoirs. They showed that a mixture of CO₂ and H₂S gives higher recovery factor
119 and more gradual pressure decline during two-cycle test compared to that of pure CO₂. They also
120 found that a mixture of CO₂-propane had the highest recovery and lowest pressure decline. The
121 recovery mechanisms that contributed to production were oil swelling and oil mobilization.

122 Injection of CO₂ under miscible and immiscible condition has been investigated in the
123 laboratory, field tests, and reservoir modeling [3, 24, 30]. In general, the results of these studies
124 indicate an increase of recovery factor for heavy and light oils cases. Field and laboratory tests
125 reported a successful immiscible CO₂ recovery in the Wilmington field (an unconsolidated
126 sandstone reservoir) [24]. Heavy oil reservoirs in the Lloydminster area are unconsolidated low-

127 pressure sandstone at depths typically between 300 and 700 m. Due to their shallow depths,
128 miscibility between oil and injected CO₂ cannot be achieved.

129 **2. Reservoir Simulation Model**

130 In this study, CO₂-based processes are evaluated as a recovery strategy for a thin heavy oil
131 reservoir. The viscosities of mixtures of the heavy oil, solution gas, and CO₂, displayed in Figure
132 1, is calculated from the log-linear mixing rule given by:

$$133 \ln \mu_{\text{mix}}(T) = x_{\text{heavy oil}} \ln \mu_{\text{heavy oil}}(T) + x_{\text{CO}_2} \ln \mu_{\text{CO}_2}(T) + x_{\text{sg}} \ln \mu_{\text{sg}}(T)$$

134 where $x_{\text{heavy oil}}$, x_{CO_2} , and x_{sg} are mole fractions of heavy oil, CO₂, and solution gas, respectively,
135 and $\mu_{\text{heavy oil}}(T)$, $\mu_{\text{CO}_2}(T)$, and $\mu_{\text{sg}}(T)$ are viscosities of the heavy oil, CO₂ (liquid equivalent), and
136 solution gas (liquid equivalent) at temperature T.

137 The reservoir model of the heavy oil formation is taken from the General Petroleum Formation
138 in the Cold Lake area of Alberta, Canada; the history-matched model used in this study is
139 described in detail in [26]. Table 1 lists properties of the reservoir model. Briefly, there are three
140 rock types derived from the logs: 1. sandstone, 2. interbedded shale, siltstone and fine-grained
141 sandstone, and 3. shale, minor siltstone and sandstone. Figure 2 displays the spatial distributions
142 of the porosity, permeability and oil saturation for the General Petroleum Formation in the area
143 of interest. The reservoir model consists of 118×147×50 gridblocks with dimensions of 20 m by
144 20 m in the horizontal directions and about 1 m in the vertical direction. A grid refinement study
145 (halving the grid in each direction) produced a 0.5% difference of results (injection and
146 production volumes) and thus the grid was considered sufficiently refined. Figure 3 displays the

147 layout of the CHOPS wells. This reservoir was under primary production (CHOPS) for ~10
148 years.

149 Following Istchenko and Gates [18], the CMG STARSTM reservoir simulator is used [10]. A
150 description of the governing equations (material balance, energy balance, diffusive and
151 convection mass transfer, multiphase flow under Darcy's law, phase behaviour and equilibrium
152 by using K-value correlations) and numerical method (finite volume method) is listed in [10].
153 The K-value correlation coefficient and other input data are listed in Table 1. The reservoir
154 simulation model includes the effects of foamy oil flow (using pseudo reactions for conversion
155 of dissolved gas to bubbles to free gas), solution gas drive, wormhole propagation, and sand
156 production (see [18] for full details). Wormholes were evolved during the CHOPS stage and they
157 are modeled as branched wells with a radius equals to 7.5 cm. The initial state of the reservoir for
158 the post-CHOPS processes is the final state of the CHOPS operation after 10 years of production
159 (see [18] for history-matched CHOPS operation). Each post-CHOPS simulation took between 10
160 and 15 hours to run on a quad core (3.4 GHz) workstation.

161 ***2.1 Post-CHOPS Cases***

162 Five cases have been investigated. Cold and hot waterflooding cases are done to establish a
163 baseline for comparison when carbon dioxide is added as an injectant to the recovery process.

164 *Case 1: Waterflooding*

165 In this process, four of the eight post-CHOPS wells are converted to injectors and the other four
166 operated as producers as shown in Figure 3. The injectors were chosen as those that were
167 perforated at relatively shallower depth to get potential benefits of gravity drainage. For

168 operating conditions, the maximum injection pressure for the injectors is 3,500 kPa, and bottom
169 hole pressure of the producers is set to 200 kPa. For the producers, an additional constraint of a
170 maximum water cut of 95% is imposed. The temperature of the water is the same as the reservoir
171 temperature (20°C).

172 *Case 2: Hot Waterflooding*

173 In this study, hot waterflooding is tested to enhance the mobility of the oil due to oil phase
174 viscosity reduction. The operating conditions and well configuration were the same as that of
175 cold waterflooding except the temperature of the injected water is equal to 200°C.

176 *Case 3: Hot Water Alternating Gas (Hot WAG)*

177 Water alternating gas injection may delay water breakthrough enabling greater oil recovery from
178 the reservoir and in turn increase oil recovery factor. In this study this process is tested as another
179 thermal recovery method hot water and carbon dioxide injected. The operating conditions and
180 well configuration are the same as that of hot waterflooding. The ratio of the injection period of
181 hot water to CO₂ is equal to 1. Over the first two years of the operation, injection periods for hot
182 water and then CO₂ were each 30 days duration. After the second year, the periods were raised
183 to 45 days.

184 *Case 4: Cyclic CO₂ Injection (CCI)*

185 Here, CO₂ is introduced into the reservoir through cyclic injection and production – each well is
186 operated cyclically (both injection and production occur in all wells). For Cyclic CO₂ Injection
187 (CCI), all of the eight wells start at the same time for the injection and production periods. For
188 operating conditions, the maximum injection pressure for cyclic processes is 4,500 kPa, and

189 producers are set to 200 kPa bottom hole pressure. For this case, each cycle is as follows: 14
190 days of CO₂ injection, 4 days of soak time, and 14 days of production for the first year. In the
191 second year, the injection and production intervals are enlarged to an injection interval of 30
192 days, and production period of 45 days.

193 *Case 5: CO₂-Hot Water Cyclic Injection*

194 To improve the energy efficiency and oil recovery, CO₂-hot water cyclic injection is tested at
195 different pressures and CO₂ volume fractions. Five tests are performed for low to high volume
196 fraction of CO₂: 25%, 50%, 75%, 99%, and 99.5% volume fraction of CO₂ at surface conditions.
197 The maximum injection pressure is equal to 4,500 kPa and the bottom hole pressure of the
198 producers is set to 200 kPa.

199 The key difference between these cases and the Hot WAG case is that these processes are cyclic
200 where the CO₂-hot water mixture is injected into the well and then fluids are produced from the
201 same well. In the Hot WAG case, slugs of each fluid are injected into the injectors and fluids are
202 produced from the producers. The length of injection and production cycles were the same as
203 that of the cyclic solvent injection case.

204 **2.2 Energy Return Ratio**

205 The performances of the different processes examined here are compared with respect to both
206 incremental recovery factor and cumulative energy efficiency (for the follow-up process only) at
207 the end of four-year post-CHOPS operation. The energy return ratio of each process (after four
208 years of operation) is defined as the ratio of the energy of the produced oil with energy value of
209 42.7 GJ/m³ to the sum of the required energy for compression (for CO₂ injection), pumping

210 water (for injection), pumping produced fluids from bottom hole to the surface (water and oil),
211 and energy requirement from burning natural gas to raise the temperature of water (for hot water
212 injection):

$$213 \text{ Energy Return Ratio} = \text{Chemical Energy of Produced Oil} / (W_p + W_c + H_{gas})$$

214 where W_p is the work of pumping water to the bottom hole and pumping liquids and sand from
215 bottom hole to the surface, W_c is the work of compressors for injection of CO₂, and H_{gas} is the
216 combustion energy of gas consumed to increase the temperature of water.

217 **3. Results and Discussion**

218 Table 2 lists a summary of the results of the cases described above. Prior to the follow-up
219 process, the cumulative energy return ratio of the cold production process was equal to 10.5 GJ
220 out per GJ invested in the recovery process. The recovery factor achieved by the cold production
221 process was equal to 10.3%. The following subsections describe the results from the cases
222 described above.

223 ***3.1 Waterflooding, Hot Waterflooding, and Hot Water-Alternating Gas***

224 For the cold waterflooding case, 124,730 m³ of water was injected into the formation and 32,167
225 m³ of heavy oil is produced. Water breakthrough, defined where the water cut at the production
226 wells reached 95%, did not occur in the four years of operation. As listed in Table 2, this process
227 results in an incremental recovery factor of 2.1% at the end of four-year process with an energy
228 return ratio of 3.8 GJ/GJ (GJ energy produced as chemical energy in the oil per GJ energy
229 consumed in the recovery process). Recovery of this process is relatively low because of the high
230 mobility ratio between the water and heavy oil phases.

231 Figure 4 compares the result of thermal and non-thermal waterflooding processes; the results
232 reveal that the incremental oil recovery has remained almost the same among these cases.
233 However, the energy return ratio of hot waterflooding is improved to 5.6 GJ/GJ from 3.8 GJ/GJ
234 for the cold waterflooding process. The reason is first due to increasing oil mobility as a result of
235 viscosity reduction due to heating. In the hot water injection case, the hot water at 200°C has
236 lower viscosity (about 0.134 cP) compared to that of the cold water (at 20°C, viscosity is 1.02
237 cP) and thus it has a faster breakthrough time at about 900 days (defined when the water cut
238 exceeded 95% at the production wells) than that of the cold water injection case.

239 The results of the Hot WAG case (water-to-gas ratio equal to 1), shown in Figure 5, reveal that
240 Hot WAG did not improve process performance compared to hot waterflooding over the period
241 of 4 years both with respect to recovery factor and energy efficiency. In the Hot WAG case, the
242 energy return ratio is slightly worse than that of the hot water flood at 5.3 GJ/GJ. This is because
243 of the lower amount of mobilized oil in the Hot WAG case as well as the additional energy
244 required to compress the CO₂ for injection into the reservoir.

245 In general, the results suggest that flood type processes (waterflood, hot waterflood, hot WAG)
246 are not good choices for post-CHOPS heavy oil reservoirs with high oil viscosity. This is due to
247 the mobility ratio of the water to heavy oil and the relatively high conductivities of the
248 wormholes that tend to convey the flooding fluid from the injector to the producer rather than
249 allowing displacement from the unrecovered regions between the wormholes.

250 ***3.2 Cyclic CO₂ Injection (CCI)***

251 As listed in Table 2, the results show 54.9 million m³ (expressed at standard conditions,
252 equivalent to ~101,900 tonnes) of CO₂ was injected into the reservoir over four years of

253 operation. As CO₂ diffuses into heavy oil, the viscosity of the oil drops and its mobility rises.
254 Furthermore, the oil phase swells which can help move oil towards the production well. The
255 results shown in Figure 5 show that for 2.4% incremental oil recovery over the four years of
256 operation, the required CO₂ volume is 61 m³/m³ of produced oil (volumes expressed at surface
257 conditions). Therefore, for the cyclic CO₂ injection design, the process requires a total CO₂ net
258 volume of 2,370,900 m³ (~4,405 tonnes) over four years of cyclic injection and up to 4.3% of the
259 total amount of CO₂ injected by volume is sequestered in the reservoir. Environmental benefits
260 by having some part of the CO₂ stored in the reservoir is attractive; however, the amount
261 sequestered within the reservoir is relatively small compared to the amount injected. The
262 cumulative oil production profile is monotonic with no reduction of the overall slope.

263 Figure 6 shows the pressure around wells in two layers at different times, in which two of them
264 have wormholes grown within these two layers. The results show that pressure depletion happens
265 around the wormholes and the zone of depleted pressure enlarges as the recovery processes
266 evolves. For the CCI process, the incremental recovery at the end of four years is 2.4% with
267 energy return ratio of 9.9 GJ/GJ. Although the incremental recovery factor is low, the energy
268 return ratio is much better than the other processes. This is because hot water is not used in this
269 process.

270 ***3.3 CO₂-Hot Water Cases***

271 The results for the cyclic CO₂ and hot water injection cases listed in Table 2 reveal that the
272 incremental recovery factor ranges from 3 to 6.6% depending on the relative amounts of CO₂ and
273 hot water. The energy return ratio for the processes range from 1.8 to 4.3 GJ/GJ with the lowest
274 achieved at a ratio of 50% CO₂ and 50% hot water. As the amount of CO₂ is raised, the energy

275 return ratio rises primarily due to the reduction of hot water injected in the process. The results
276 suggest that there is an optimum value with respect to the CO₂-hot water ratio that balances the
277 incremental recovery factor and the energy return ratio. Since the amount of oil produced in the
278 25% CO₂ and 75% hot water case is relatively large, its energy return ratio is slightly larger than
279 that of the 50% CO₂/50% hot water case. As the hot water content drops, the energy invested in
280 the process drops and thus for processes with greater than 50% CO₂, the energy return ratio rises
281 despite the lower amount of oil produced.

282 The results shown in Figure 7 for the 25% CO₂-75% hot water and 99% CO₂-1% hot water cases
283 reveal the net CO₂ stored in the reservoir is relatively low. The lower the amount of water
284 injected, the smaller is the cumulative oil produced. The cumulative oil profiles are monotonic
285 and do not demonstrate a reduction of their slope which indicates that further operation beyond
286 the four years evaluated here would yield significantly greater oil volumes. By increasing the
287 CO₂ volume fraction, the total incremental recovery decreases but the energy efficiency of the
288 processes increases. The best case among these CO₂-hot water cases reveals that about 4.1% of
289 the CO₂ volume injected is sequestered in the reservoir. Again, similar to the CCI results, the
290 relative amount of CO₂ stored is small.

291 Figure 8 displays the temperature distribution around the wells for the 25% CO₂-75% hot water
292 case. The results show that for most of the wells, the temperature directly within the wormhole
293 networks is partially heated due to the cyclic injection and production. The addition of CO₂
294 reduces the amount of heat convected into the reservoir. The largest heated zone surrounding a
295 well occurs for Well 12 (leftmost, bottom well) – in this well, the size of the heated zone reaches
296 about 90 m in diameter and the heated zone extends beyond the wormhole network.

297 *3.4 Discussion: Energy Efficiency Analysis and Carbon Dioxide Storage*

298 A comparison of the energy return ratios of the processes considered here is presented in Figure
299 9. The results show that the CCI process yields the greatest energy return ratio with hot water
300 flood at about two-thirds of the CCI value. The reason that hot waterflooding yields a relatively
301 high energy return ratio is due to due to the relatively small amount of hot water injected which
302 leads to a relatively large mobilization of oil. CO₂ enables much more oil from the reservoir but
303 with a reduction of the energy return ratio. Design of such processes with CO₂-hot water can
304 decrease the viscosity of the oil far from the wormholes as hot water loses its heat at a larger
305 distance away from the wellbore and swelled oil with reduced viscosity flows to the production
306 wells in a post-CHOPS reservoir.

307 As presented in Table 2, the 25% CO₂-75% hot water process gives the highest incremental
308 recovery factor for CO₂-based processes for the reservoir in this study with final oil recovery of
309 102,150 m³ after four years of post-CHOPS. However, its energy return ratio is not high.

310 The results suggest that CO₂ is a practical choice given its favourable energy efficiency. Among
311 the proposed steam-CO₂-based processes, the CO₂-steam/hot water injection (case of 25% CO₂-
312 75% hot water) has the highest recovery factor and acceptable energy efficiencies although its
313 cumulative steam-to-oil ratio is relatively high (5.7 m³/m³). The CO₂-steam/hot water injection
314 (case of 99% CO₂-1% hot water) has an energy efficiency of 3.0 (GJ out/GJ in) and lower
315 cumulative hot water-to-oil ratio (4.1 m³/m³) which is favourable, it results in an incremental
316 recovery factor of 3.6%.

317 The results reveal that the opportunity for CO₂ sequestration in the reservoir during the post-
318 CHOPS oil recovery processes considered here is small, typically less than 10%. The reason for

319 this is that the amount of water in the system is not large and thus the capability to store CO₂ is
320 small. Also, for cyclic processes, each production period is a blowdown step which largely
321 produces back most of the injected CO₂ due to the pressure drop that occurs on production.
322 Injecting hot water raises the temperature of the system which consequently lowers the solubility
323 of CO₂ within the fluids in the reservoir and thus, co-injection of CO₂ and hot water does not
324 provide optimal conditions for storage of CO₂ in the formation. This suggests that CO₂-based
325 processes are not good candidates for CO₂ sequestration during oil recovery.

326 **4. Conclusions**

327 There is a potential to recover incremental oil from reservoirs that have been operated under
328 primary production cold heavy oil production with sand (CHOPS) by using CO₂. CO₂ has a high
329 injectivity value and it is used under immiscible conditions which enables its penetration into the
330 reservoir through wormholes. It also yields a reduction of heavy oil viscosity and oil swelling
331 within the reservoir.

332 Waterflooding and water alternating gas do not perform as well as CO₂ injection due to high
333 viscosity of the oil for the post-CHOPS reservoir in this study. Therefore, CO₂ cyclic injection
334 alone or with hot water can be optimized to improve recovery from the reservoir. With CO₂
335 cyclic injection, the incremental recovery factor at the end of four years of operation is 2.4%
336 with relatively high energy efficiency; the energy return ratio is the highest of all of the processes
337 evaluated here. Cyclic solvent injection with hot water appears to be a reasonable option with
338 incremental recovery factor equal to 6.6% for the best case. However, the energy return ratio of
339 CO₂-hot water injection for the reservoir is relatively low compared to the other cases examined

340 here. The amount of CO₂ sequestered within the reservoir during the CO₂-based recovery
341 processes is relatively small, usually less than 5%.

342 **Acknowledgements**

343 Authors would like to thank the financial support of the Petroleum Technology Research Centre
344 Saskatchewan (PTRC) for this project, and Computer Modeling Group Ltd. for the use of their
345 thermal reservoir simulation software CMG STARS™. We would also like to thank Jacky Wang
346 for his help and comments on the modeling part of this study.

347 **References**

- 348 1. Adams, D.M., 1982. Experiences with waterflooding Lloydminster heavy-oil reservoirs.
349 J. Can. Pet. Technol., 34(8):1643-1650, doi: <http://dx.doi.org/10.2118/10196-PA>.
- 350 2. Asghari, K., Nakutnyy, P., 2008. Experimental results of polymer flooding of heavy oil
351 reservoirs. Paper presented at the 2008 Canadian International Petroleum Conference,
352 Calgary, Alberta, Canada; 17-19 June, doi: <http://dx.doi.org/10.2118/2008-189>.
- 353 3. Asghari, K., Torabi, F., 2008. Effect of miscible and immiscible CO₂ flooding on gravity
354 drainage experimental and simulation results. Paper presented at the 2008 SPE
355 Symposium on Improved Oil Recovery, Tulsa, Oklahoma, USA 20-23 April, doi:
356 <http://dx.doi.org/10.2118/110587-MS>.
- 357 4. Belgrave, J. D. M., Moore, R. G., Ursenbach, M. G., and Bennion, D. W., 1993. A
358 comprehensive approach to in-situ combustion modeling. SPE Adv. Technol. Series,
359 1(1):98-107, doi: <http://dx.doi.org/10.2118/20250-PA>.
- 360 5. Cenovus Energy, 2013. Annual Performance Report available at www.aer.ca.

- 361 6. Chang, J., Ivory, J., 2013. Field-scale simulation of cyclic solvent injection (CSI). *J. Can.*
362 *Pet. Technol.*, 52(4):251-265, doi: <http://dx.doi.org/10.2118/157804-MS>.
- 363 7. Chang, J., Ivory, J., 2014. Predictive field-scale simulations for the design of a solvent
364 injection pilot. Paper presented at the 2014 SPE Heavy Oil Conference, Calgary, Alberta,
365 Canada, 10-12 June, doi: <http://dx.doi.org/10.2118/170134-MS>.
- 366 8. Chen, J., Coates, R., Oldakowski, K., Wiwchar, B., 2014. In situ combustion as a follow-
367 up process to CHOPS. Paper presented at the 2014 SPE Heavy Oil Conference, Calgary,
368 Alberta, Canada 12-14 Jun, doi: <http://dx.doi.org/10.2118/157847-MS>.
- 369 9. CNRL, 2014. Annual Performance Report available at www.aer.ca.
- 370 10. Computer Modelling Group Ltd. 2015, STARS™ User Manual.
- 371 11. Denbina, E.S., Baker, R.O., Gegunde, G.G., Klesken, A.J., Sodero, S.F., 2001. Modelling
372 cold production for heavy oil reservoirs. *J. Can. Pet. Technol.*, 40(3):23-29, doi:
373 <http://dx.doi.org/10.2118/01-03-01>.
- 374 12. Dong, M, Ma, S., Liu, Q., 2009. Enhanced heavy oil recovery through interfacial
375 instability: a study of chemical flooding for Brintnell heavy oil. *Fuel*, 88(6):1049-1056,
376 doi: 10.1016/j.fuel.2008.11.014.
- 377 13. Dusseault, M., 1993. Cold production and enhanced oil recovery. *J. Can. Pet. Technol.*,
378 32(9):16-18, doi: <http://dx.doi.org/10.2118/93-09-01>.
- 379 14. Gates, I.D., 2010. Solvent-aided steam-assisted gravity drainage in thin oil sand
380 reservoirs. *J. Pet. Sci. Eng.*, 74(3-4):138-146, doi: <http://dx.doi.org/10.2118/130443-PA>.
- 381 15. Gates, I.D., Larter, S.R., 2014. Energy efficiency and emissions intensity of SAGD. *Fuel*,
382 115:706-713, doi: 10.1016/j.fuel.2013.07.073.

- 383 16. Gao, C.H., 2011. Advances of polymer flood in heavy oil recovery. Paper presented at
384 the 2011 SPE Heavy Oil Conference and Exhibition, Kuwait City, Kuwait; 12-14
385 December.
- 386 17. Huerta, M., Alvarez, J.M., Jossy, E., Forshner, K., 2012. Use of acid gas (CO₂/H₂S) for
387 the cyclic solvent injection (CSI) process for heavy oil reservoirs. Paper presented at the
388 2012 SPE Heavy Oil Conference, Calgary, Alberta, Canada, 12-14 June, doi:
389 <http://dx.doi.org/10.2118/157825-MS>.
- 390 18. Istchenko, C.M., Gates, I. D., 2014. Well/Wormhole model of cold heavy oil production
391 with sand. SPE J., 19(2):260-269, doi: <http://dx.doi.org/10.2118/150633-PA>.
- 392 19. Kantzas, A., Brook, G., 2004. Preliminary laboratory evaluation of cold and post-cold
393 production methods for heavy oil reservoirs part B, reservoir conditions. J. Can. Pet.
394 Technol., 43(10):39-48, doi: <http://dx.doi.org/10.2118/04-10-04>.
- 395 20. Li, H., Zheng, S., Yang, D., 2013. Enhanced swelling effect and viscosity reduction of
396 solvent(s)-CO₂-heavy oil systems. SPE J., 8(4):695-707.
- 397 21. Maini, B.B., 1999. Foamy oil flow in primary production of heavy oil under solution gas
398 drive. Paper presented at the 1999 SPE Annual Technical Conference and Exhibition, 3-6
399 October, Houston, Texas, USA.
- 400 22. Maini, B.B., Sarma, H.K., George, A.E., 1993. Significance of foamy oil behavior in
401 primary production of heavy oils. J. Can. Pet. Technol., 32(9):50-54, doi:
402 <http://dx.doi.org/10.2118/93-09-07>.
- 403 23. Miller, K.A., 2006. Improving the state of the art of Western Canadian heavy oil water
404 flood technology. J. Can. Pet. Technol., 45(4):7-11, doi: [http://dx.doi.org/10.2118/06-04-](http://dx.doi.org/10.2118/06-04-GE)
405 GE.

- 406 24. Saner W.B., Patton, J.T., 1986. CO₂ recovery of heavy oil: Wilmington field test. *J. Pet.*
407 *Technol.*, 38(7):769-776, doi: <http://dx.doi.org/10.2118/12082-PA>.
- 408 25. Shah, A., Fishwick, R., Wood, J., Leeke, G., Rigby, S., Greaves, M., 2010. A review of
409 novel techniques for heavy oil and bitumen extraction and upgrading. *Energy Environ.*
410 *Sci.*, 3:700-714.
- 411 26. Sharifi Haddad, A., Gates, I.D., 2015. Modelling of cold heavy oil production with sand
412 (CHOPS) using a fluidized sand algorithm. *Fuel*, 158:937-947, doi:
413 [10.1016/j.fuel.2015.06.032](http://dx.doi.org/10.1016/j.fuel.2015.06.032).
- 414 27. Tremblay, B., Sedgwick, G., Forshner, K., 1996. Imaging of sand production in a
415 horizontal sand pack by X-ray computed tomography. *SPE Form. Eval.*, 11(02): 94-98,
416 doi: <http://dx.doi.org/10.2118/30248-PA>.
- 417 28. Tremblay, B., Sedgwick, G., Forshner, K., 1997. Simulation of cold production in heavy
418 oil reservoirs: wormhole dynamics. *SPE Reservoir Eval.*, 12(02):110-117, doi:
419 <http://dx.doi.org/10.2118/35387-PA>.
- 420 29. Tremblay, B., Sedgwick, G., Forshner, K., 1998. Modelling of sand production from
421 wells on primary recovery. *J. Can. Pet. Technol.*, 37(3):41-50, doi:
422 <http://dx.doi.org/10.2118/98-03-03>.
- 423 30. Zhang, Y.P., Huang, S.S., Luo, P., 2010. Coupling immiscible CO₂ technology and
424 polymer injection to maximize EOR performance for heavy oils. *J. Can. Pet. Technol.*,
425 49(5):25-33, doi: <http://dx.doi.org/10.2118/137048-PA>.
- 426 31. Zhao, W., Wang, J., and Gates, I.D, 2014. Thermal recovery strategies for thin heavy oil
427 reservoirs. *Fuel*, 117:431–441, doi: <http://dx.doi.org/10.1016/j.fuel.2013.09.023>.

428 32. Zhao, W., Wang, J., and Gates, I.D., 2013. Optimized solvent-aided steam-flooding
429 strategy for recovery of thin heavy oil reservoirs. *Fuel*, 112:50-59,
430 doi:10.1016/j.fuel.2013.05.025.

431 **Table 1: Properties of Cold-Lake CHOPS reservoir used in the simulation model. Source of**
 432 **data is Reference [26] unless otherwise noted.**

Property	Value																																																
Depth to reservoir top (m)	291																																																
Net pay (m)	~6																																																
Porosity	0.06-0.40																																																
Oil saturation	0.4-0.8																																																
Solution gas-to-oil ratio (m ³ /m ³)	10																																																
Horizontal rock permeability k _h (mD)	30-8500																																																
k _v /k _h	0.8																																																
Effective rock compressibility (1/kPa)	5x10 ⁻⁶																																																
Rock heat capacity (kJ/m ³ °C)	2,600																																																
Rock thermal conductivity (kJ/m day °C)	660																																																
Reference pressure (kPa)	2,500																																																
Reference depth (m)	291																																																
Initial reservoir temperature, °C	20																																																
Dead oil viscosity (cP)	See Figure 1																																																
Water viscosity	Correlation listed in [10]																																																
Liquid equivalent solution gas viscosity (cP)	See Figure 1																																																
Correlation: $\mu = Ae^{\frac{B}{T}}$																																																	
Gas phase viscosity (cP)	0.00864 (1.574 + 0.0044·T(°C)) (from [10])																																																
Oil phase density, kg/m ³	$\frac{920}{e^{0.0007(T-T_{ref})(°C) + 7 \times 10^{-7}(P-P_{ref})(kPa)}}$, (T _{ref} = 15.5 °C and P _{ref} = 1 atm)																																																
Water phase density	Correlation listed in [10]																																																
Gas phase density	Redlich-Kwong equation of state with zero interaction coefficients [10]																																																
Water thermal conductivity (kJ/m day °C)	53.4																																																
Gas thermal conductivity (kJ/m day °C)	5																																																
Oil thermal conductivity (kJ/m day °C)	11.5																																																
Foamy-oil kinetic parameters	N ₁ =1.44 1/day, N ₂ =0.288 (gmol/m ³) ² /day, G ₁ =0 1/day, G ₂ =0.23 (gmol/m ³) ² /day (from [18])																																																
Liquid phase diffusion coefficient (carbon dioxide), m ² /s	1.9×10 ⁻⁹																																																
Liquid phase diffusion coefficient (methane), m ² /s	1.5×10 ⁻⁹																																																
K-values (methane) = $\frac{Kv1}{P} e^{\left(\frac{Kv4}{T(C)-Kv5}\right)}$	Kv ₁ =5.4547×10 ⁵ kPa, Kv ₄ =-879.84°C, Kv ₅ =-265.99°C																																																
K-values (carbon dioxide) = $\frac{Kv1}{P} e^{\left(\frac{Kv4}{T(C)-Kv5}\right)}$	Kv ₁ =8.6212×10 ⁵ kPa, Kv ₄ =-3103.39°C, Kv ₅ =-272.99°C																																																
Wormhole radius (m)	0.075																																																
Number of gridblocks	118 × 147 (horizontal) × 50 (vertical)																																																
Dimensions of gridblocks (m)	20 × 20 (horizontal) × 1 (vertical)																																																
Oil-water relative permeability curves	<table border="1"> <thead> <tr> <th>S_w</th> <th>k_{rw}</th> <th>k_{row}</th> <th></th> </tr> </thead> <tbody> <tr><td>0.2000</td><td>0.0000</td><td>0.7000</td><td></td></tr> <tr><td>0.3750</td><td>0.0000</td><td>0.2759</td><td></td></tr> <tr><td>0.5500</td><td>0.0000</td><td>0.0658</td><td></td></tr> <tr><td>0.5969</td><td>0.0014</td><td>0.0376</td><td></td></tr> <tr><td>0.6125</td><td>0.0031</td><td>0.0303</td><td></td></tr> <tr><td>0.6594</td><td>0.0148</td><td>0.0139</td><td></td></tr> <tr><td>0.6750</td><td>0.0215</td><td>0.0101</td><td></td></tr> <tr><td>0.7063</td><td>0.0402</td><td>0.0047</td><td></td></tr> <tr><td>0.7531</td><td>0.0839</td><td>0.0007</td><td></td></tr> <tr><td>0.7844</td><td>0.1252</td><td>0.0000</td><td></td></tr> <tr><td>0.8000</td><td>0.1500</td><td>0.0000</td><td></td></tr> </tbody> </table>	S _w	k _{rw}	k _{row}		0.2000	0.0000	0.7000		0.3750	0.0000	0.2759		0.5500	0.0000	0.0658		0.5969	0.0014	0.0376		0.6125	0.0031	0.0303		0.6594	0.0148	0.0139		0.6750	0.0215	0.0101		0.7063	0.0402	0.0047		0.7531	0.0839	0.0007		0.7844	0.1252	0.0000		0.8000	0.1500	0.0000	
S _w	k _{rw}	k _{row}																																															
0.2000	0.0000	0.7000																																															
0.3750	0.0000	0.2759																																															
0.5500	0.0000	0.0658																																															
0.5969	0.0014	0.0376																																															
0.6125	0.0031	0.0303																																															
0.6594	0.0148	0.0139																																															
0.6750	0.0215	0.0101																																															
0.7063	0.0402	0.0047																																															
0.7531	0.0839	0.0007																																															
0.7844	0.1252	0.0000																																															
0.8000	0.1500	0.0000																																															
Gas-Liquid relative permeability curves	<table border="1"> <thead> <tr> <th>S_l</th> <th>k_{rg}</th> <th>k_{rog}</th> <th></th> </tr> </thead> <tbody> <tr><td>0.4000</td><td>0.5000</td><td>0.0000</td><td></td></tr> <tr><td>0.5000</td><td>0.2560</td><td>0.0000</td><td></td></tr> <tr><td>0.6000</td><td>0.1080</td><td>0.0000</td><td></td></tr> <tr><td>0.6563</td><td>0.0579</td><td>0.0046</td><td></td></tr> <tr><td>0.6750</td><td>0.0456</td><td>0.0109</td><td></td></tr> <tr><td>0.7125</td><td>0.0264</td><td>0.0369</td><td></td></tr> <tr><td>0.7500</td><td>0.0135</td><td>0.0875</td><td></td></tr> <tr><td>0.8063</td><td>0.0033</td><td>0.2275</td><td></td></tr> <tr><td>0.8625</td><td>0.0000</td><td>0.4689</td><td></td></tr> </tbody> </table>	S _l	k _{rg}	k _{rog}		0.4000	0.5000	0.0000		0.5000	0.2560	0.0000		0.6000	0.1080	0.0000		0.6563	0.0579	0.0046		0.6750	0.0456	0.0109		0.7125	0.0264	0.0369		0.7500	0.0135	0.0875		0.8063	0.0033	0.2275		0.8625	0.0000	0.4689									
S _l	k _{rg}	k _{rog}																																															
0.4000	0.5000	0.0000																																															
0.5000	0.2560	0.0000																																															
0.6000	0.1080	0.0000																																															
0.6563	0.0579	0.0046																																															
0.6750	0.0456	0.0109																																															
0.7125	0.0264	0.0369																																															
0.7500	0.0135	0.0875																																															
0.8063	0.0033	0.2275																																															
0.8625	0.0000	0.4689																																															

Table 2: Summary of results of cases investigated (after four years of operation). For the follow-up processes, the incremental RF and cumulative quantities are over the duration of the follow-up process (does not include initial cold production process).

Process	Cum. Oil Prod. (m³)	Cum. Water Inj. (m³)	Cum. CO₂ Inj. (Sm³)	RF%	Cum. Energy Return Ratio (GJ out/GJ in)	Cum. HWOR (m³/ m³)
Cold Production	158,614	-	-	10.3	10.5	-
Follow-up Process	Cum. Oil Prod. (m³)	Cum. Water Inj. (m³)	Cum. CO₂ Inj. (Sm³)	Incremental RF%	Cum. Energy Return Ratio (GJ out/GJ in)	Cum. HWOR (m³/ m³)
Waterflooding	32,167	124,730	-	2.1	3.8	-
Cyclic CO ₂ Injection (CCI)	38,837	-	54,858,100	2.4	9.9	-
Hot Waterflooding	31,004	67,510	-	2.0	5.6	2.1
Hot WAG, ratio = 1	29,100	27,963	1,482,660	1.9	5.3	1.0
CO ₂ -Hot Water, Ratio 25:75	102,146	586,675	195,500	6.6	2.0	5.7
CO ₂ - Hot Water, Ratio 50:50	88,943	576,116	576,090	5.6	1.8	6.5
CO ₂ -Hot Water, Ratio 75:25	64,543	421,685	1,265,050	4.0	1.9	6.5
CO ₂ -Hot Water, Ratio 99:1	56,476	231,750	22,943,200	3.6	3.0	4.1
CO ₂ -Hot Water, Ratio 99.5:0.5	48,343	122,320	24,341,800	3.0	4.3	2.5

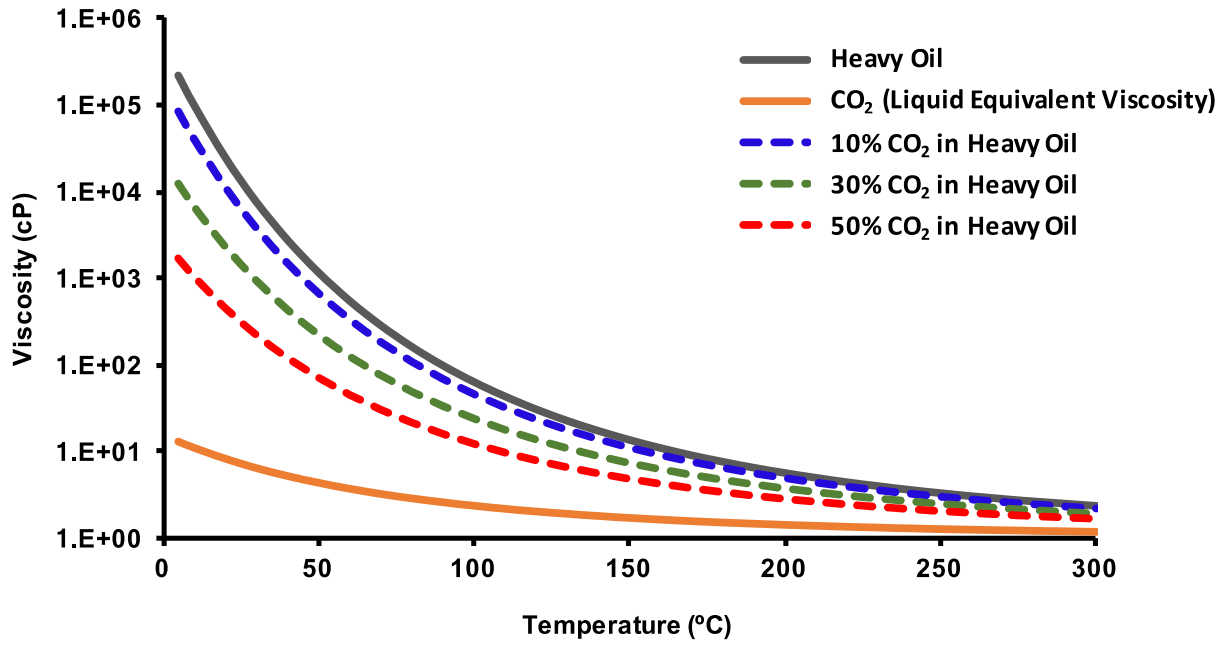


Figure 1: Viscosity of heavy oil and CO₂ (as equivalent liquid phase, solution gas has same liquid equivalent viscosity) and their mixtures (mole percent) in the reservoir model.

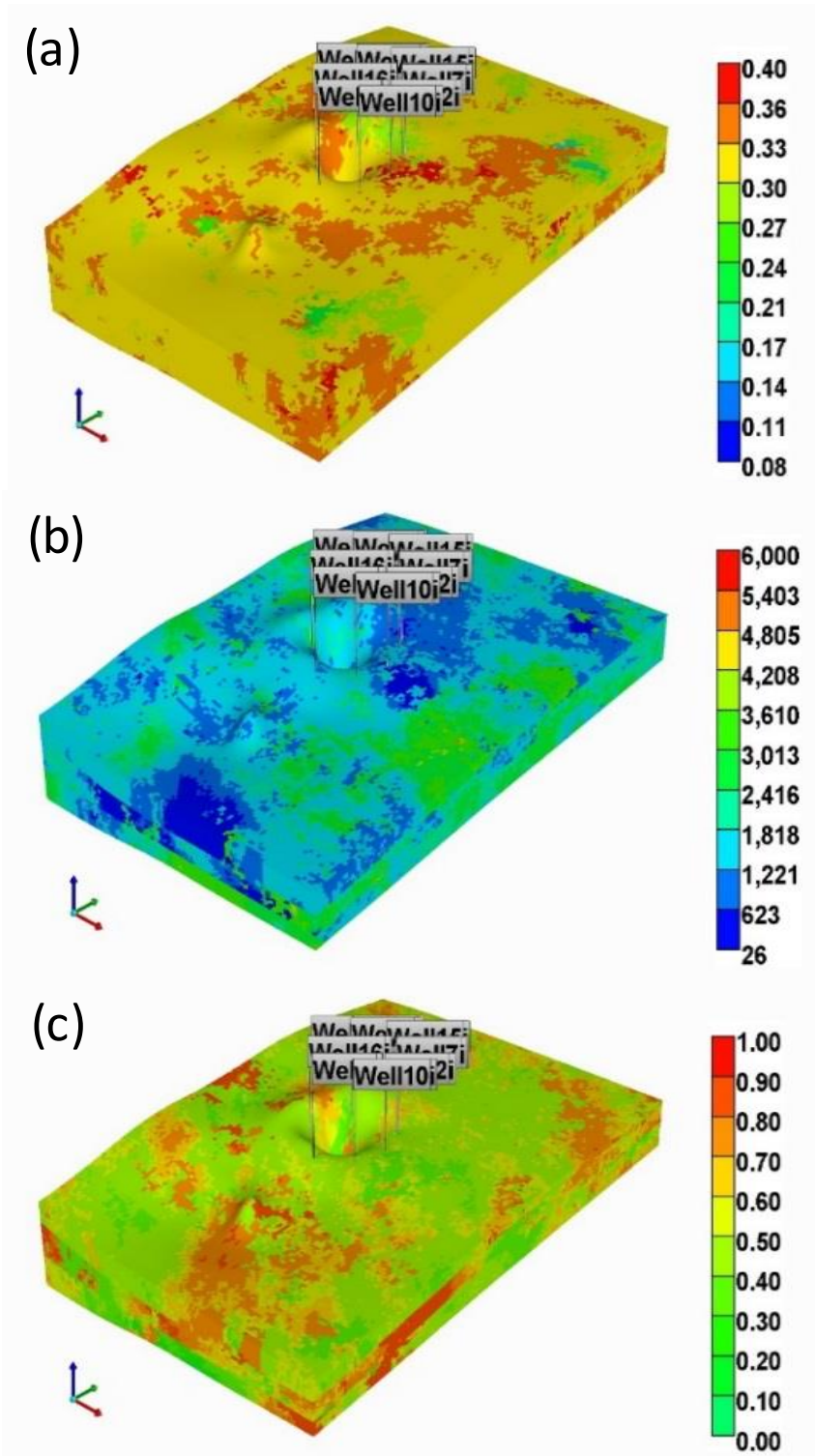


Figure 2: (a) Porosity, (b) permeability, and (c) oil saturation at the start of the post-CHOPS process. Average porosity is equal to 35% and horizontal permeability is between ~100 mD and ~8 D.

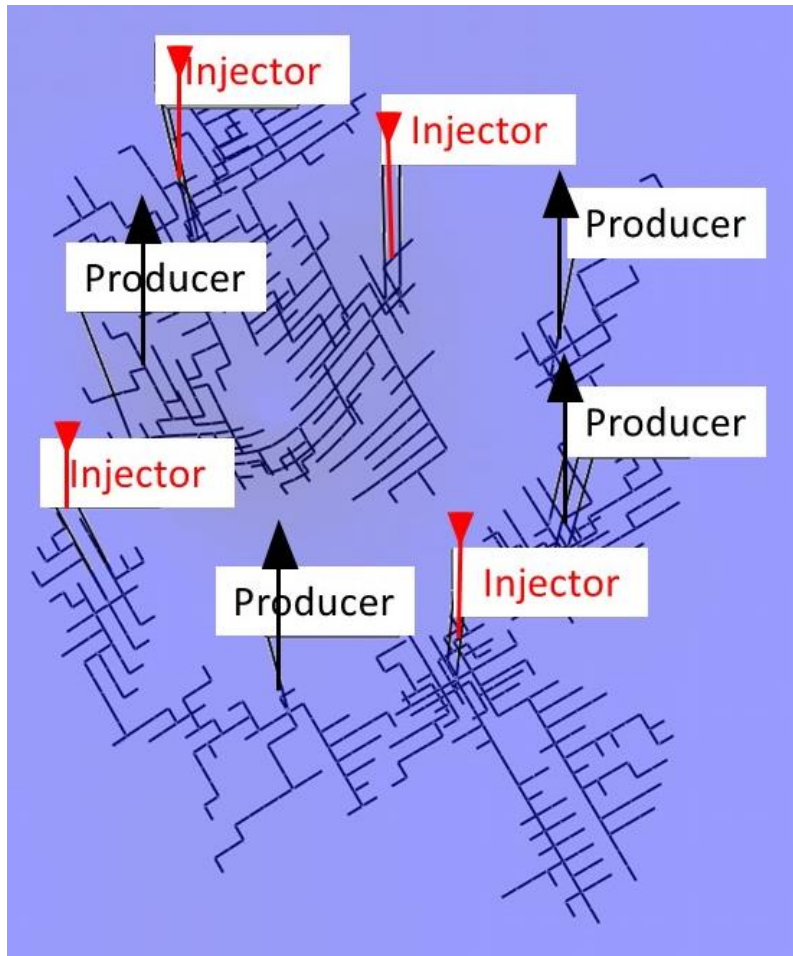


Figure 3: Arrangement of injector and producer wells used in waterflood, hot waterflood and hot WAG processes.

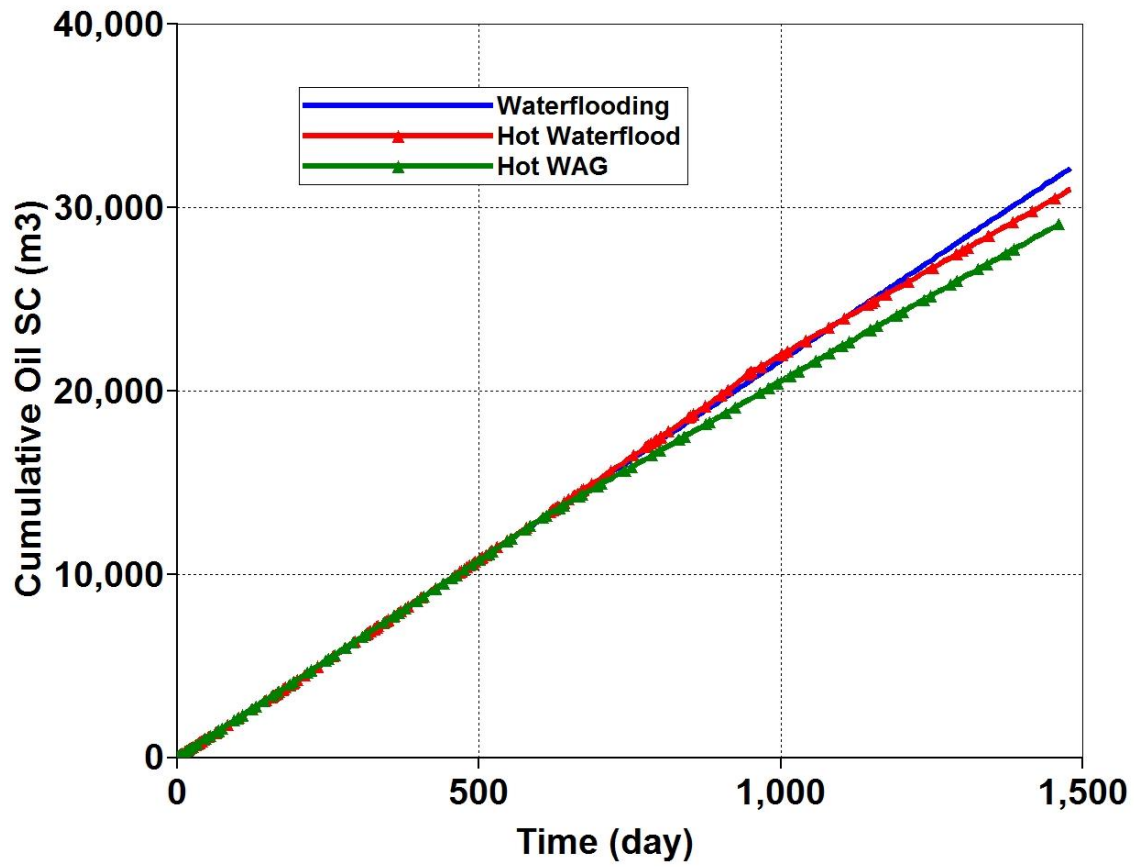


Figure 4. Performance of water flood and hot water alternating CO₂ (Hot WAG) cases.

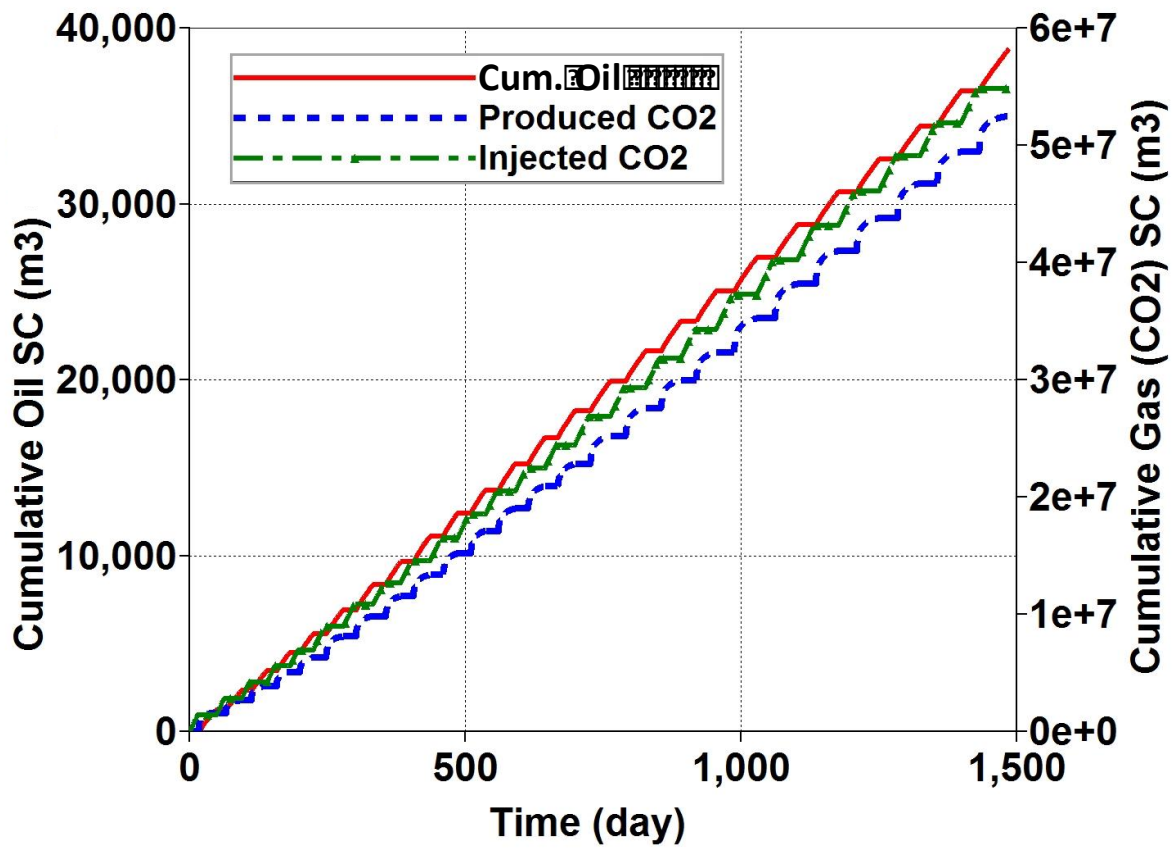
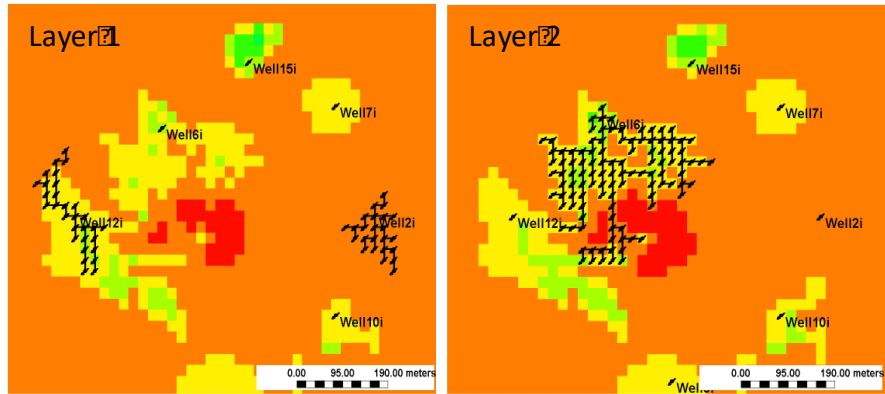
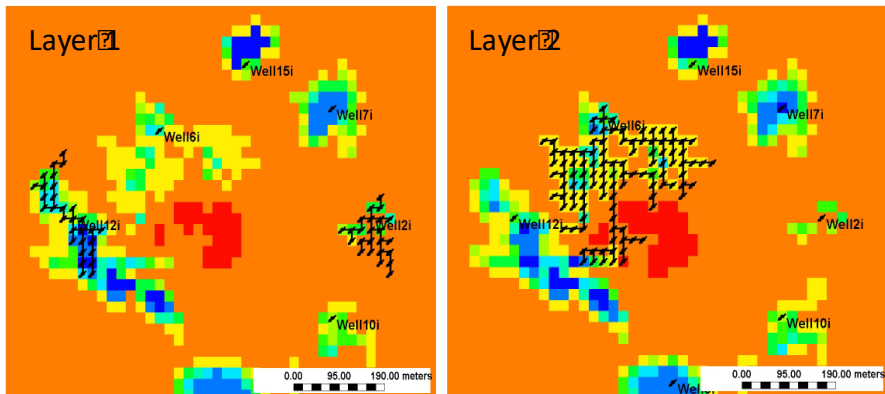


Figure 5. Cumulative oil recovered with CCI and the volume of injected and produced CO₂.

End of CHOPS



After 6 Months post-CHOPS



End of Last Injection Cycle (1440 days post-CHOPS)

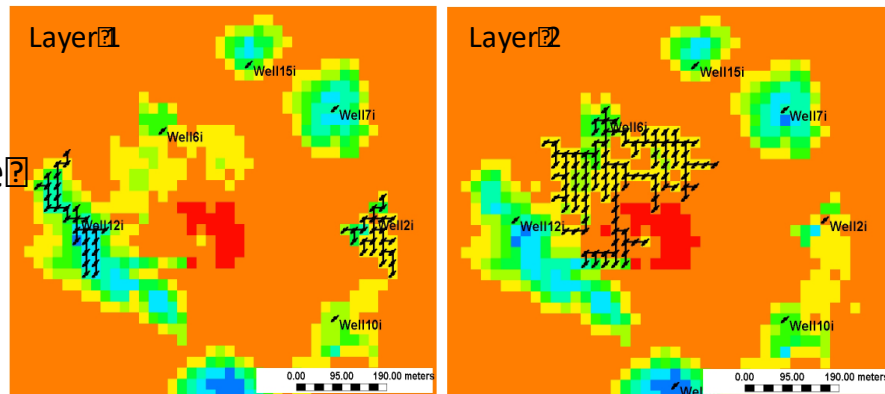


Figure 6. Pressure (kPa) distribution in two consecutive layers for the cyclic CO₂ injection process at start of post-CHOPS operation, after 6 months post-CHOPS operation, and end of last injection cycle (1440 days).

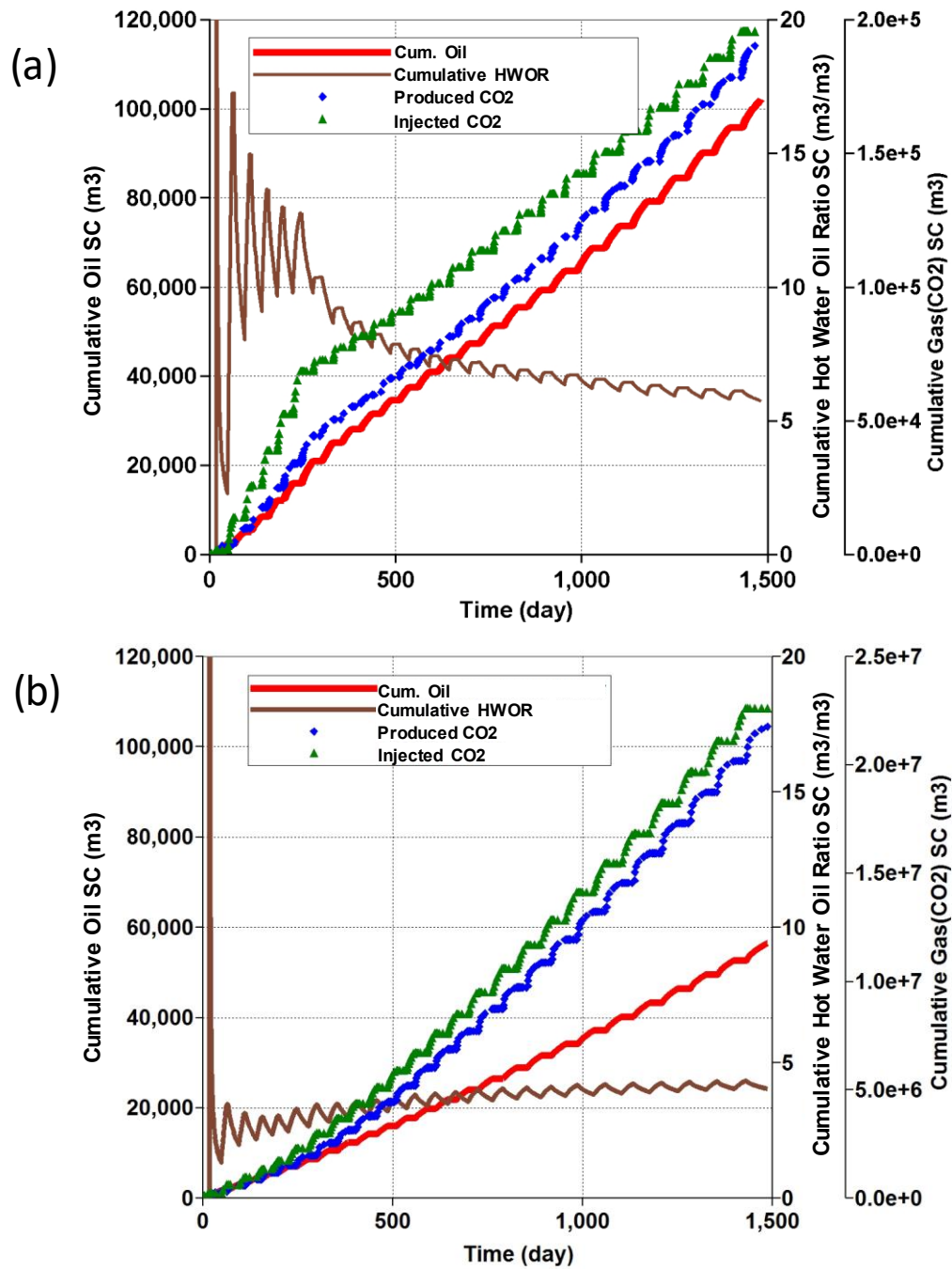
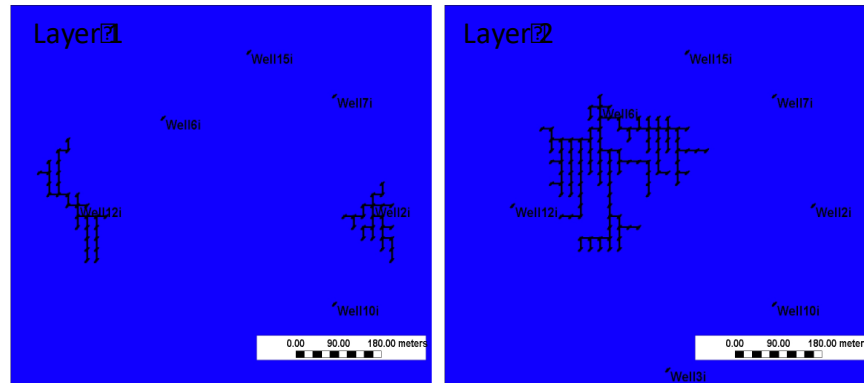
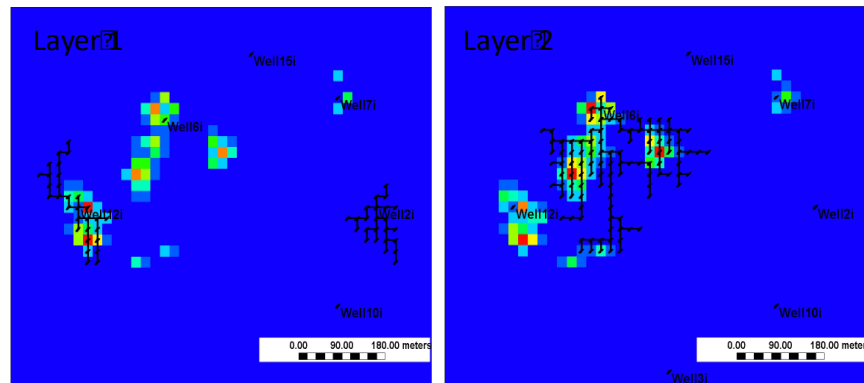


Figure 7. Cumulative oil recovered for cyclic CO₂-Hot Water stimulation cases, hot water-to-oil ratio, and CO₂ injected and produced: (a) CO₂-Water ratio: 25:75 and (b) CO₂-Water ratio: 99:1.

End of CHOPS



After 6 Months post-CHOPS



End of Last Injection Cycle (1440 days post-CHOPS)

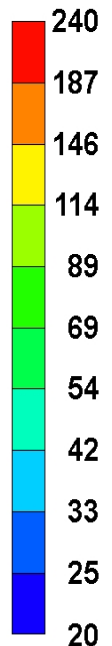
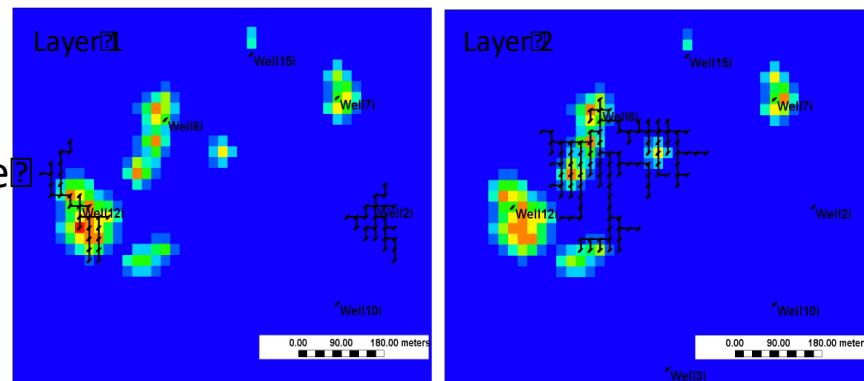


Figure 8. Temperature ($^{\circ}\text{C}$) distribution in two consecutive layers for cyclic CO_2 -hot water stimulation (CO_2 -Water ratio: 25:75) at (a) start of post-CHOPS, (b) after 6 months, (c) end of last injection cycle (1440 days).

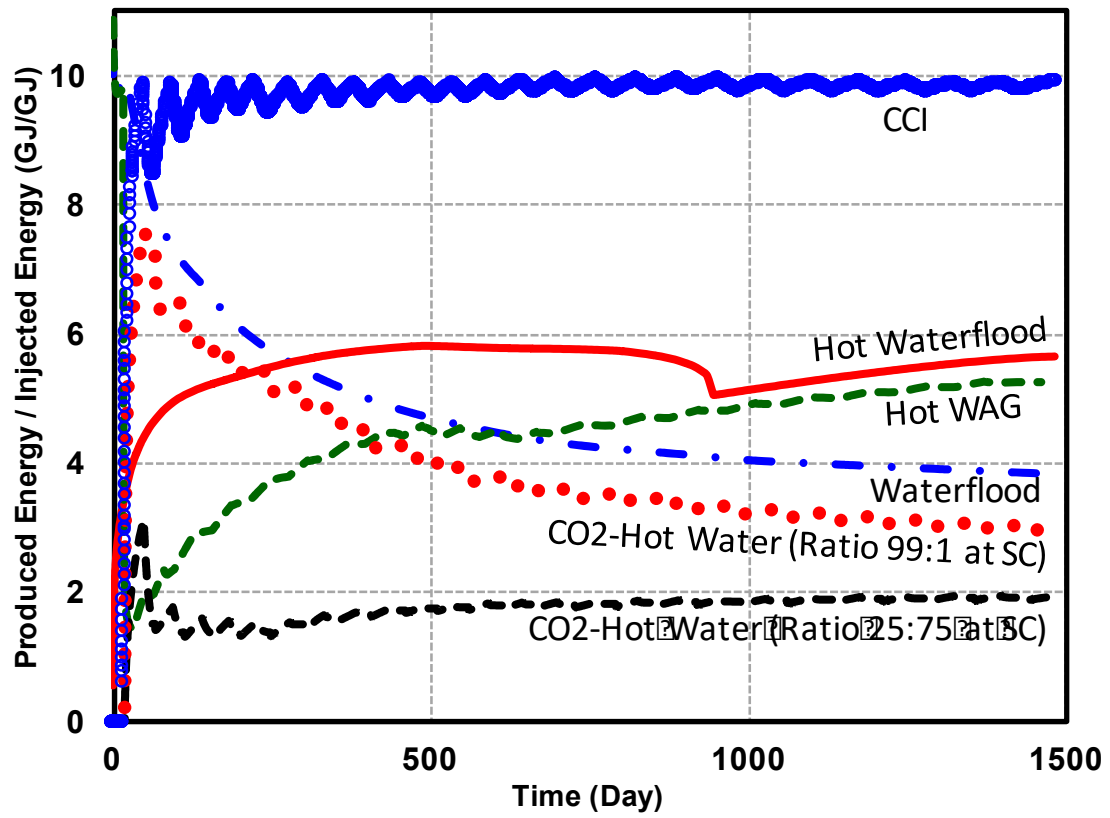


Figure 9. Energy return ratios of different post-CHOPS processes.